www.sciencemag.org/cgi/content/full/1147880/DC1

Supporting Online Material for

A β-Defensin Mutation Causes Black Coat Color in Domestic Dogs

Sophie I. Candille, Christopher B. Kaelin, Bruce M. Cattanach, Bin Yu,
Darren A. Thompson, Matthew A. Nix, Julie A. Kerns, Sheila M. Schmutz,
Glenn L. Millhauser, Gregory S. Barsh*

*To whom correspondence should be addressed. E-mail: gbarsh@stanford.edu

Published 18 October 2007 on *Science* Express

DOI: 10.1126/science.1147880

This PDF file includes:

Materials and Methods
SOM Text
Figs. S1 to S10
Tables S1 to S3
References

Supporting Material

Materials and Methods

Genome sequence

Throughout this paper the dog genome assembly used is CanFam1.0 as displayed and annotated in the UCSC genome browser, http://genome.cse.ucsc.edu/ (*1*). During the course of this work, a second assembly of the dog genome became available, CanFam2.0 (*2*), in which the last 5 Mb of CFA16, where the *K* locus maps, are inverted compared to CanFam1.0. However, the linkage map (*3*), two radiation hybrid maps (*4, 5*), a FISH map (*5*) and our own mapping data support the CanFam1.0 orientation. Therefore we conclude that the correct orientation is that of the CanFam1.0 sequence and all the map coordinates in this manuscript are presented according to the CanFam1.0 sequence.

Dog DNA samples and skin biopsies collection

Catch-All swabs (Epicenter) or Cytopak brushes (Medical Packaging) were used to collect cheek swab samples through the mail or at dog shows according to a Stanford IACUC-approved protocol. DNA from the swabs was prepared using the Qiamp DNA mini kit (Qiagen). Skin biopsies from dogs euthanized for purposes unrelated to this study were obtained from a local animal shelter.

Genotyping and sequencing

Microsatellite markers are given in Table S1, and were identified before the dog genome assembly was released by blast-searching the dog trace archive at NCBI, http://www.ncbi.nlm.nih.gov/Traces, with repeat-masked human sequence from the regions of predicted homology on human chromosomes 4 and 8. SNP and indel markers were identified by sequencing amplicons designed to validate SNPs from the dog genome variation database (*2*), or by resequencing as depicted in Figure 2.

SNP genotyping and sequencing of PCR-amplified genomic DNA was carried out using standard fluorescent dye terminator technology on a capillary instrument, and analyzed using CodonCode Aligner 1.5.1c (CodonCode Corporation) or Sequencher 4.2 (Gene Codes Corporation). Microsatellite genotyping of PCR-amplified genomic DNA was carried out by incorporating a fluorescent primer in the PCR reaction or by using a fluorescently labeled universal primer as described by Travis Glenn at the University of Georgia DNA Lab, http://www.uga.edu/srel/DNA_Lab (*6*), and calling genotypes with GeneMapper software (Applied Biosystems). Primer sequences for polymorphisms on CFA16 are given in Tables S1 and S2, including those used to genotype *CBD103*ΔG23, referred to as S54 in Table S2. Genotyping of the R96C mutation in *Agouti* and the R306ter mutation in *Mc1r* has been described previously (*7, 8*).

Genetic data analysis

Statistical tests of association and LD plots as shown in Figure 1 were carried out with Haploview (*9*). The markers depicted in Figure 1 do not significantly deviate ($p>0.001$) from Hardy-Weinberg expectations (a requirement for accurate implementation of the allelic association test). However, the Bonferroni-corrected thresholds depicted in Figure 1 should be viewed as a general guide rather than absolute tests of significance for individual SNPs because

many of the SNPs are correlated, and because of the potential for varying degrees of relatedness among some samples. Haplotypes were estimated using Phase v2.1 (*10*). For estimation of haplotype-sharing and inferring the position of ancestral recombination events (Figures 2, S5, S9, S10), missing genotypes and apparent double recombination events within less than 1 kb (which are most likely due to gene conversion) were ignored.

RT-PCR and qRT-PCR

Skin biopsies from euthanized dogs were immersed in RNAlater (Ambion) and stored at -80ºC. After thawing, total RNA was isolated by homogenization with a rotor-stator and extraction using the RNeasy Fibrous Tissue Midi kit (Qiagen). Each RT or qRT-PCR reaction was carried out with 1 ug of total RNA. Primers were designed for each of the 16 beta-defensin genes on CFA16, the 4 beta-defensin genes on CFA25, *Agouti*, and *Bactin* as a reference, and are available on request.

Expression of *CBD103* in transgenic mice and in keratinocytes

For transgenic mice, protein-coding sequences for *CBD103* or *CBD103GΔ23* were PCR-amplified from genomic DNA, cloned into an EcoRI site in the pCAGGS expression vector, which drives transgenic expression under the regulation of a cytomegalovirus/beta-actin hybrid (CAGGS) promoter (*11*). During PCR amplification, we used primer sequences (5'-ACTGGAATTCGCCGCCACCATGAGGATCTATTACCTTCTCCTCC-3' and 5'-ACTGGAATTCCCCATCCCATTTCTGGATTT-3') to incorporate an extended Kozak sequence to improve translation efficiency. The transgene was excised by digestion with SalI and BamHI, gel-purified, and subsequently microinjected into (FVB/N x C57BL6/J) F1 one cell embryos by the Stanford Transgenic Facility. Potential founder mice were genotyped by PCR using the following primers 5'-CGTGCTGGTTATTGTGCTGT-3' and 5'-CCTGCACCTGAGGAGTGAAT-3'.

For transfection of a mouse keratinocyte cell line (generously provided by Dr. Tony Oro, Department of Dermatology, Stanford University), protein-coding sequences for CBD103 or CBD103Δ23 were PCR-amplified from the transgenic constructs using the following primers, 5'-ACTGCTCGAGGCCGCCACCATGAGGATCTATTACCTTCTCCTCC-3' and 5'-ACTGTTCGAATTTCTTTCTTCGGCAGCATTT-3', then cloned as C-terminal fusion proteins into the pcDNA 3.1/V5-His A plasmid (Invitrogen) using XhoI and BstBI.

Keratinocytes were grown in 154CF medium supplemented with 0.2mM $CaCl_2$ and human keratinocyte growth supplement (Cascade Biologics), and transfected using the Fugene HD reagent (Roche Applied Science) in 6 well plates. 48 to 72 hours post-transfection, the proteins were extracted from both the cells and the media using a protocol adapted from (*12*). Media was collected and centrifuged for 20 min (all centrifugations were at 4ºC and 20,000g), and the supernatant precipitated using trichloroacetic acid. The cell layer was washed twice with cold PBS, scraped into 1M HCl and sonicated, then centrifuged for 10 min. The pellet was then reextracted with 5% acetic acid and spun down for 10 minutes. The HCl and acetic acid extracts were pooled and lyophilized. Proteins precipitated from the media, or lyophilized from the acid extract of the cell layer, were dissolved in 40 ul of Novex tricine SDS sample buffer (Invitrogen) prior to SDS-polyacrylamide gel electrophoresis under reducing conditions on a 16% Novex tricine gel (Invitrogen). After electrophoresis and transfer to nitrocellulose, the membrane was

blocked in 5% milk and hybridized overnight at 4ºC with a monoclonal anti-V5 antibody (Invitrogen) in 2.5% milk. (Equal protein loading was checked by staining the membrane using the Memcode stain (Pierce). An HRP-conjugated anti-mouse antibody (Biorad) was used as a secondary antibody and hybridized for 1 hour, then developed with the ECL substrate (GE Healthcare). The loading control, beta-actin, was subsequently detected using a monoclonal anti-β-actin antibody (Sigma), and the same secondary antibody.

This experiment was repeated 4 times; each experiment included 3 – 4 independent transfections of the *CBD103* and *CBD103GΔ23* constructs. Our conclusion that more CBD103GΔ23 than CBD103 accumulates in the media is based on the Cochran-Mantel-Haenszel Chi-Square test, comparing the relative levels of the two proteins across all 4 experiments.

Peptide synthesis

All peptides were produced on an Applied Biosystems 433A peptide synthesizer using standard Fmoc chemistry. Amino acids were purchased from NovaBiochem and assembled on Rink-amide-MBHA resin. Pre-activated Fmoc-Cys(Trt)-OPfp was used to avoid enantiomerization. Coupling reactions used four equivalents of each amino acid in N, N,-Dimethyl Formamide (DMF), along with O-Benzotriazole-N,N,N',N'-tetramethyl-uronium-hexafluoro-phosphate (HBTU) and N, N-Diisopropylethylamine (DIEA) except Pre-activated Fmoc-Cys(Trt)-OPfp which was only coupled in DMF solution. Fmoc protecting groups were removed using a 1% mixture of 1,8-diazabicyclo[5.4.0]undec-7-ene and Hexamethyleneimine. Cleavage was performed in a mixture of Trifluoroacetic acid/Triisopropylsilane/1, 2-Ethanedithiol/phenol (90:4:4:2) for 90 min. Oxidative folding was achieved by dissolving peptides to a concentration of 0.1mg/mL in folding buffer (0.5-1.0 M Guanidine hydrochloride, 0.1 M Tris, 1.0 mM reduced Glutathione, 0.1 mM oxidized glutathione, pH 8.5) with stirring for 48 hours. Folding was monitored by HPLC, and gave rise to one, or sometimes two, closely migrating but distinct major peaks. In cases where two major peaks were observed (for CBD103ΔG23 and HBD1), the pharmacologic behavior and mass of the material from the different peaks was identical, suggesting that the different peaks represented non-covalent conformers, as we have previously described for a synthetic version of Agouti protein (*13*). The folded products were purified by HPLC using a C18 column and identified as fully oxidized peptides by mass spectrometry (accurate to within 1.0 amu). Accurate concentrations were determined with amino acid analysis performed at the molecular structure facility at UC Davis.

We note that Wu et al. (*14*) described structural studies of HBD1, HBD2, and HBD3, in which HBD1 and HBD2 were found to fold easily into a single species but HBD3 was not. We did not observe any difficulty in obtaining a single folded species of HBD3, perhaps because we used a different folding protocol.

cAMP and receptor-ligand binding assays

Melan-A cells (*15*) were grown in RPMI supplemented with 200nM TPA at 37ºC and 10% CO2. Prior to each assay, cells were plated onto 96-well half-area plates (Corning #3885) at a density of 20,000 cells/well and grown for 24 hours. After washing the wells once with PBS, pH 7.4, peptides (diluted in PBS, pH7.4, containing 0.2% BSA and 0.5 mM IBMX) were added and the plate was incubated at 37ºC and 10% CO2 for 40 minutes. cAMP levels were measured using the

Hithunter cAMP XS kit (DiscoverX) and a Centro LB 960 plate reader (Berthold Technologies). All assays were carried out in triplicate and analyzed using Graphpad (Prism).

All receptor-ligand binding assays were performed using DELFIA lanthanide-based detection system on intact 293T cells transiently transfected with melanocortin receptor expression constructs. The human Mc1r and human Mc4r constructs were generously provided by Dr. Ying-Kui Yang (Department of Pediatric Surgery, University of Alabama, Birmingham); the dog and mouse Mc1r constructs were made by cloning the protein-coding regions PCR-amplified from genomic DNA into the pcDNA3.1(-) vector (Invitrogen).

For binding assays, a 10 cm dish of 293T cells was transfected with 10 ug of a melanocortin receptor expression construct using calcium phosphate, with transfection efficiency monitored by parallel transfection with a GFP-tagged Mc4r construct. After 12 - 16 hours, the media was changed, and at 24 hours the cells were trypsinized, washed once in media, and resuspended in binding buffer, then added to a 96-well Acrowell filtration plate (Pall).

For saturation binding, 2/3 serial dilutions of Europium-labelled NDP-MSH (Eu-NDP-MSH, Perkin-Elmer) were added to individual wells and incubated for 2 hours at 37ºC. To measure non-specific binding, a similar dilution series of Eu-NDP-MSH was added in the presence of 1.5 uM of unlabelled NDP-MSH. For displacement binding, a tracer level of Eu-NDP-MSH (1.8 – 3.0 nM) was added together with varying concentrations of ASIP-YY or a defensin peptide. After the incubation, binding buffer was filtered by centrifugation, wells were washed three times with 200 ul ice-cold wash buffer, and 150 ul of enhancement solution (Perkin-Elmer) was added to each well. The plates were then incubated at room temperature for 45 minutes and time-resolved fluorescence measured using a FluoStar Optima plate reader (BMG Labtech). The conditions for the binding assays with regard to the number of cells (20,000 – 70,000 per well) and the concentration of Eu-NDP-MSH (1.8 – 3.0 nM) were based on pilot experiments estimating both Bmax and Ki, and adjusted to maintain an appropriate dynamic range, and avoid depletion of free ligand by more than 10%. The time and temperature used for the binding assay were based on pilot experiments and recommendations from Perkin-Elmer regarding conditions required to reach binding equilibrium with Eu-NDP-MSH. Data shown in Table 1 are based on 13 experiments in which multiple ligands were tested with multiple receptors in each experiment. Data were fit with a sigmoidal dose response curve with variable slope and analyzed using Graphpad.

For studying a potential interaction between CBD103 and ASIP-YY, we preincubated varying concentrations of ASIP-YY with 50 nM CBD103, and used the mixture in a displacement binding assay. In this paradigm, if CBD103 functions solely as a competitive ligand for Mc1r, then a mixture of CBD103 and ASIP-YY will behave additively with regard to Eu-NDP-MSH displacement, apparent as a reduction in the maximal Eu-NDP-MSH binding, and a slight leftward shift in the binding curve. However, if CBD103 binds to and sequesters ASIP-YY, the mixture of CBD103 and ASIP-YY will cause a rightward shift in the displacement curve.

Supporting Text

<u>Linkage and association mapping</u>

The 12 Mb interval to which we previously mapped the K^B mutation (*16*) is defined by markers REN292N24 and FH3592 (Figure S1). We ascertained additional kindreds segregating K^B, k^{br}, and k^y; among a total of 151 meioses from 8 breeds, we identified 22 chromosomes recombinant

between the *K* locus and markers located in the original 12 Mb interval that were obtained from the RH map (*4*) or developed from the dog genome sequence (markers M1 – M12, Table S1). Four of these recombinant chromosomes, 1 from a k^{br}/k^{y} parent, and 3 from a K^{B}/k^{y} parent, define the smallest interval by linkage analysis that contains the *K* locus. Pedigrees and genotypes are shown in Figures S2 – S4, and delineate overlapping critical regions of 3.8 Mb and 7.6 Mb for the K^{B} and k^{br} mutations, respectively (Figure S1).

For association mapping, we chose to first examine Boxers, because brindle vs. yellow is a simple dominant trait that involves only the *K* locus, and because Boxers exhibit relatively long haplotype blocks (*2*); both features increase the power to detect association. In this manuscript we use the term "yellow" to refer to any pheomelanic dog; however, most dog breeders distinguish between "yellow" vs. "fawn", referring to colors caused by $Mc1r^{e}$ vs. the combination of a^{y} and k^{y}. Although there is specificity for some breeds with regard to which alleles segregate (e.g. fawn Boxers and fawn Great Danes never carry $Mc1r^{e}$), the genotypes cannot be distinguished simply on the basis of phenotype. For the purposes of consistency, therefore, we use the term "yellow" to refer to a pheomelanic color in all breeds, with the understanding that within the dog breeding community, the same animal might be described as fawn (e.g. a Boxer or Great Dane). These issues are discussed further by Kerns et al. (*16*) and Berryere et al. (*17*).

Within the 3.8 Mb interval defined by recombination, we identified 267 polymorphisms with a targeted resequencing strategy. A subset of these polymorphisms were genotyped on 10 yellow (k^{y}/k^{y}) vs. 12 brindle (k^{br}/k^{br} or k^{br}/k^{y}) Boxers, and revealed a broad peak of significant association (Bonferroni-corrected p value <0.05) across 1.9 Mb (Figures 1A, 1C). We then tested 10 black (K^{B}/K^{B}, K^{B}/k^{br}, or K^{B}/k^{y}) vs. 9 yellow (k^{y}/k^{y}) Great Danes, and identified a more restricted peak of significant association across 320 kb (Figure 1C). The difference in the size of the regions between breeds correlates with the differences in linkage disequilibrium (LD) structure; in Boxers, highly correlated SNP pairs ($r^2=1$) are found up to 1.1 Mb apart, compared to 60 kb apart in Great Danes (Figure S5).

The 320 kb region of significant association in Great Danes focused our attention on the beta-defensin cluster as candidate genes; sequencing the mature protein-coding regions for 9 members of the cluster in 3 k^{y}/k^{y} animals (2 Boxers, 1 Great Dane) and 2 K^{B}/K^{B} animals (Great Dane, Labrador Retriever) revealed several polymorphisms concordant with the K^{B} allele, including the ΔG23 mutation in *CBD103*. We then genotyped ΔG23, 2 additional SNPs in *CBD103*, and 30 SNPs in the surrounding 1 Mb in 9 yellow and 11 black dogs from 12 different breeds. The ΔG23 polymorphism was again completely concordant with the K^{B} allele, and together with the 2 additional SNPs in *CBD103*, revealed a highly significant association ($p < 10^{-6}$) only at the 3 *CBD103* polymorphisms.

For the large 38 breed study, we classified dogs into two categories with regard to their putative *K* locus genotype. In the presence of functional *Agouti* and *Mc1r* alleles, the K^{B} allele causes exclusive production of eumelanin in areas that contain pigment cells; therefore black, chocolate, brown, liver, blue, harlequin, mantle, bicolor (black and white), and spotted black dogs should be heterozygous or homozygous for K^{B} (*16*). Conversely, the k^{y} allele permits production of pheomelanin in some or all body regions depending on the genotype of *Agouti*; therefore yellow, fawn, red, apricot, cream, wheaten, tricolor (black, yellow and white), black-and-tan, tan point, and sable dogs should be homozygous for k^{y}. Among 454 dogs, there were 13 cases where the ΔG23 polymorphism did not correlate with coat color phenotype (Table S3), but could be explained by known epistatic interactions: 5 “black” animals (in the German Shepherd Dog or

Weimaraner breeds) were homozygous for a loss-of-function *Agouti* allele, and 8 "yellow" animals (in the Afghan Hound, French Bulldog, German Shorthaired Pointer, Labrador Retriever, Puli, or Poodle breeds) were homozygous for a loss-of-function *Mc1r* allele.

Short-range resequencing and haplotype studies

We resequenced all non-repetitive regions in a 20 kb interval surrounding *CBD103* in 5 yellow and 5 black dogs representing 7 breeds, and identified 28 polymorphisms (22 SNPs and 6 indels including the ΔG23 polymorphism) at a frequency > 0.2, that were then used to infer short-range haplotypes. Along with the 6 "parental" k^y-bearing and 5 "parental" K^B-bearing chromosomes (depicted in yellow and blue, respectively, Figure 2A), 3 chromosomes carrying a single ancestral recombinant event defined a proximal boundary for K^B 7.69 kb 5' of the ΔG23 mutation (Figure 2A).

To define a distal boundary, we tested 44 additional K^B/k^y dogs representing 14 breeds for a SNP that lay 9.65 kb distal to the ΔG23 mutation (S103, Figure 2A and Table S2), and identified 5 dogs, all Great Danes, that were homozygous for the k^y-associated S103 variant. Further genotyping revealed that 4 of the recombinant chromosomes define a distal boundary for K^B 1.46 kb 3' of the ΔG23 mutation (Figure 2A). Thus, the maximal interval for K^B defined by haplotype analysis is 9146 bp, and contains both exons of *CBD103*, the first exon of dog EST CX990240 and dog EST C0665262 (Figure 2B).

The K^Bmutation and pharmacology of Mc1r signaling

The genetic data indicating that CBD103ΔG23 is the cause of the K^B mutation is conclusive, but its precise mechanism of action is not. Because CBD103 and CBD103ΔG23 bind competitively and with high affinity to the dog Mc1r, they have the potential to displace Agouti protein, which normally serves as an "endogenous antagonist"—or, more formally, an inverse agonist—of the Mc1r. From this perspective, a plausible model is that the dog Mc1r, in the absence of any ligand, has sufficiently high levels of basal activity to promote eumelanin production, that Agouti protein acting as an inverse agonist depresses that basal activity to elicit pheomelanin production, and that CBD103ΔG23 acting as a neutral antagonist prevents Agouti protein from binding to the Mc1r, thereby restoring high levels of basal activity to the Mc1r. However, our results (and the aforementioned model) do not exclude the possibility that CBD103 or CBD103ΔG23 may cause the Mc1r to couple to a G protein alpha subunit other than Gs, such as Gi or Gq. In either case, the biochemical mechanism of the K^B mutation—loss of the N-terminal glycine from the mature CBD103 protein—may cause a black coat color by increasing the affinity for the Mc1r, increasing availability of the mature protein in vivo, or both.

Based on solution structures of other beta-defensins (*18*), the N-terminal glycine of the mature CBD103 peptide (Gly23) lies in a region that is unstructured, and it is not immediately apparent why loss of this glycine—leading to an N-terminal isoleucine—should cause an ~5-fold increase in affinity for the dog Mc1r. In any case, our results suggest that the core beta-defensin fold is an important determinant of the high-affinity binding we observed between beta-defensins and the Mc1r, since the primary sequence of HBD1 is very different from that of HBD3 (the human ortholog of CBD103). Distinguishing among these possibilities may be possible with additional structural studies of beta-defensins, melanocortin receptors, or both.

Evolution of *K* locus haplotype structure and breed origins

The haplotype analysis presented in Figure 2 focuses on short-range haplotype structure to identify ancestral recombinants. In retrospect, knowing that the ΔG23 mutation in *CBD103* is the K^B mutation allowed an evaluation of long-range haplotype structure in Boxers and Great Danes, which revealed some interesting correlations with breed history. Although most breeds were formally established late in the 19th century, there is wide variation in the time at which typical characteristics for specific breeds appear in historical records. In particular, dogs similar in morphology to Great Danes can be recognized in records from the Middle Ages and earlier, while dogs similar in morphology to Boxers were not evident until much later (*19*). Using genotype data from the association study (Figure 1), we inferred haplotypes within a 2.6 Mb region surrounding the *K* locus for 12 brindle (5 k^{br}/k^{br} and 7 k^{br}/k^{y}) and 9 yellow (k^{y}/k^{y}) Boxers, and for 10 (7 K^B/K^B and 3 K^B/k^y) black and 9 yellow (k^y/k^y) Great Danes (Figures S9, S10).

In Boxers, all 17 k^{br} chromosomes share a single long haplotype, 618 – 991 kb, centered on *CBD103*, whereas the 25 k^y chromosomes have multiple haplotypes over the same region (Figures S5, S9). Furthermore, haplotype diversity in the 2.6 Mb region surrounding *CBD103* is greater in Boxer k^y chromosomes than in Boxer k^{br} chromosomes (Figure S9). Records from the first Deutscher Boxer Club show in 1896 (*20*) show both brindle and yellow dogs; thus, both alleles were represented early in breed derivation. Taken together, these observations suggest that k^{br} is a recent mutation that occurred prior to breed formation, and predict that differences between k^{br} and k^y haplotypes in Boxers will be found in other breeds that segregate brindle.

In Great Danes, the single haplotype shared by 17 K^B chromosomes is 13 – 93 kb (Figure S10), considerably shorter than the k^{br}-associated haplotype in Boxers (Figure S9). Furthermore, haplotype diversity is similar in K^B and k^y chromosomes in Great Danes with 1.5 and 1.9 chromosomes per haplotype respectively (Figure S10). Both observations are consistent with a longer history and/or less stringent population bottlenecks in Great Danes relative to Boxers. Overall our data indicate that the ΔG23 mutation probably arose in the ancestral dog population, estimated to carry haplotype blocks on the order of 10 kb (*2*), which is consistent with the 9 kb haplotype shared by 53 K^B chromosomes from 12 breeds around *CBD103* (Figure 2). In fact, a black dog with harlequin markings—a black and white pattern that requires the K^B allele—is drawn on the Beni Hasan tomb of Khnumhotep II, with an estimated age of 1800 – 2000 B.C.

Table S1: Microsatellite markers

Marker	CFA16 (bp) CanFam1.0	Primer F	Primer R	Size (bp)
REN292N24	45414007	GCCCTCAAGCTCAATCTACG	TGCAACAGTCAAGACATGGA	141
M1	49652784	TGTCTGAACATGAACTGCATCA	AGGGTTCAGGCTCACAAAAC	238
M2	49802408	CCATCCAAATTTCTGAGTGC	GCAGTTAAGGGTCTGCCTTG	209
FH2155-a	52719635	TCAATTCCTTTGAAGCCAGTTT	AACAAAAAGTTGATAGTACATTTTCCT	308
FH2155-b	52719635	TGTAGATGATGGAGACATTGGG	AGGCAAATATGCCAAGGATG	498
M3	52732889	ACCACAAGGGCACAGACACT	TGAGCTCCAAACCAACAGACT	249
M4	52736072	AGAGCAACATTCGCAGTCAG	TTTGAAATTGAAAGCAATCATCT	157
M5	54857328	CCTCTTGTGACAGGATCAGG	GCACATTAGCCTTTCCCTTC	222
M6	54881106	GTTCCTCCATTGTCCCTGAA	AGCATCTGGATTGCCAGAAA	211
M7	54910722	TCCTGCATCCTTATTTCCAGTT	CTCCAGGAAGCAAGCAAAAC	179
M8	55029560	AGCTCCATCCAGGTTGTTTG	GGAAGCAGCCAAGTATCCAT	211
M9	55089638	CTGGGATCGAGTTCCACATC	TCCAGGGACATCCTGTAGGT	226
FH2990	55596137	GGTTGGGAATTTCTTACTGG	CTTGCTCAGCTGGAGACC	455
REN96I08	55661755	CTTAAGTGAAATGGCAATAGG	AGGGAGCTGAATGGATGAT	211
M10	56504030	CCTCCTTGGGCAGACTTCTT	TACAGGCAGTGCCAGCTCTA	164
M11	56594012	GGGGGAAAAATAGCTTCCTG	ATGACCAAACGTTGCCTAGC	209
M12	56603029	TGGGAATGAGAGAAAAAGGAA	CTGGACTCCAAAGAGGATGC	247
FH3388	57317253	TCAGAAGGTGCTCATATTTTCC	TAATTGAACCCACAACTTGG	255
FH2764	57333658	ATATGCACGTCAGCACATTC	TGTCACAGAAGTGGTTTTGC	151
FH3592	57475457	AGGTGCTGAGCATGTTATCC	TGGTCTGTGTGTGAGGAGAAA	344

Table S2: SNPs and indel polymorphisms

ID	CFA16 (bp) CanFam1.0	Tasha's allele	Other allele	Broad SNP ID	Primer Forward	Primer Reverse
S1	53971555	T	C		TGCTGCTACACTGCGTTACC	ATGGCAGATGCCCTTTACAC
S2	53971607	T	C		TGCTGCTACACTGCGTTACC	ATGGCAGATGCCCTTTACAC
S3	53971621	T	C	BICF235J3047	TGCTGCTACACTGCGTTACC	ATGGCAGATGCCCTTTACAC
S4	53971625	A	T or del		TGCTGCTACACTGCGTTACC	ATGGCAGATGCCCTTTACAC
S5	54258844	T	C		CTCAGGAGGCTGCTATCTGG	GCCATACACAGGTGCCTCTT
S6	54258880	T	A		CTCAGGAGGCTGCTATCTGG	GCCATACACAGGTGCCTCTT
S7	54258888	C	T		CTCAGGAGGCTGCTATCTGG	GCCATACACAGGTGCCTCTT
S8	54258951	C	T	BICF237J56729	CTCAGGAGGCTGCTATCTGG	GCCATACACAGGTGCCTCTT
S9	54258960	G	C		CTCAGGAGGCTGCTATCTGG	GCCATACACAGGTGCCTCTT
S10	54650550	G	C		CACCATTCGTGGGAGAAAGT	GCTCAATGGGCATTTTGTCT
S11	54650563	G	C		CACCATTCGTGGGAGAAAGT	GCTCAATGGGCATTTTGTCT
S12	54650581	G	A		CACCATTCGTGGGAGAAAGT	GCTCAATGGGCATTTTGTCT
S13	54650600	A	G		CACCATTCGTGGGAGAAAGT	GCTCAATGGGCATTTTGTCT
S14	54650616	A	G	BICF231J58300	CACCATTCGTGGGAGAAAGT	GCTCAATGGGCATTTTGTCT
S16	55217908	G	A	BICF233J59359	ATGGAGATGGGTGAGAGTGG	GCATGGAAACAGCAATCTGA
S17	55218721	C	T		TCTTGCTTTGAAATCTCTCTTCA	TGCACAGTCAGTTCCATCCT
S18	55218747	C	A		TCTTGCTTTGAAATCTCTCTTCA	TGCACAGTCAGTTCCATCCT
S19	55218887	T	C		TCTTGCTTTGAAATCTCTCTTCA	TGCACAGTCAGTTCCATCCT
S20	55371177	A	C		GGGTGAAATCCACCAGATTG	CACAAATCAAGCTGCGAATC
S21	55371224	A	G	BICF237J39766	GGGTGAAATCCACCAGATTG	CACAAATCAAGCTGCGAATC
S22	55541817	G	C	BICF237J64796	TAGAAAAATGCCCCATTTGC	CTTTCTGAGCCGAGTCCTTG
S23	55541842	C	T		TAGAAAAATGCCCCATTTGC	CTTTCTGAGCCGAGTCCTTG
S24	55541843	T	G		TAGAAAAATGCCCCATTTGC	CTTTCTGAGCCGAGTCCTTG
S25	55541844	G	T		TAGAAAAATGCCCCATTTGC	CTTTCTGAGCCGAGTCCTTG
S26	55541858	G	T		TAGAAAAATGCCCCATTTGC	CTTTCTGAGCCGAGTCCTTG
S27	55548577	G	A		GAAAGTAAGGCCCTGTGTGC	AGGATCATGCCTTCCAACAG
S28	55548600	C	T	BICFPJ214189	GAAAGTAAGGCCCTGTGTGC	AGGATCATGCCTTCCAACAG
S29	55548608	C	G		GAAAGTAAGGCCCTGTGTGC	AGGATCATGCCTTCCAACAG
S30	55551795	C	G		GGACCTAATTCTCAGCCAGG	GGTGATCTCACCTCGCTTGT
S31	55551944	G	C		GGACCTAATTCTCAGCCAGG	GGTGATCTCACCTCGCTTGT
S32	55551952	C	T	BICFPJ547724	GGACCTAATTCTCAGCCAGG	GGTGATCTCACCTCGCTTGT
S33	55551998	T	G		GGACCTAATTCTCAGCCAGG	GGTGATCTCACCTCGCTTGT
S34	55581684	A	G		TCCTTCAGTCATTCTTACTCATTTG	TCAGACTTCACTGGGGTTTTC
S35	55581728	T	C		TCCTTCAGTCATTCTTACTCATTTG	TCAGACTTCACTGGGGTTTTC
S36	55585724	C	T		GACCCTGAGTCTGCACCTCT	GGAAAACAAAAATCGCAAGAA
S37	55585819	C	G	BICFPJ767999	GACCCTGAGTCTGCACCTCT	GGAAAACAAAAATCGCAAGAA
S38	55585840	T	C		GACCCTGAGTCTGCACCTCT	GGAAAACAAAAATCGCAAGAA
S39	55709569	T	G	BICF233J60510	ATCCACCAGCACCTTCTCAG	TAGTCAGGGTTGGGAACTGG
S40	55714953	C	T		TACGAAAGAAACCCGTGTCC	CAGCTCCTGCTAAGCCACTT
S41	55725863	A	T	BICFPJ945361	GTGGTGACCAGGGAAGGTAG	ACTCTGCTGTGAGCTGGGTT
S42	55726825	G	A		TCCATAAATGGGTAGTTGTGCTT	ATTTTTCCAAAGTTCGGGGT
S43	55726868	T	C	BICFPJ945365	TCCATAAATGGGTAGTTGTGCTT	ATTTTTCCAAAGTTCGGGGT
S44	55726885	G	C		TCCATAAATGGGTAGTTGTGCTT	ATTTTTCCAAAGTTCGGGGT

Table S2 (cont.): Polymorphisms used in the association study of the *K* locus

ID	CFA16 (bp) CanFam1.0	Tasha's allele	Other allele	Broad SNP ID	Primer Forward	Primer Reverse
S45	55740429	A	G		AGCCTACAGAGGCAGGATGA	CTGGCTTAGGGACACACCTC
S46	55742802	C	T		AGCGCTATGAACACAAGGGT	TGGAGGACATATTTGTGTTTGTG
S47	55742803	C	A		AGCGCTATGAACACAAGGGT	TGGAGGACATATTTGTGTTTGTG
S48	55742826	C	T	BICFPJ70048	AGCGCTATGAACACAAGGGT	TGGAGGACATATTTGTGTTTGTG
S49	55754820	G	A		TCTGCCTTTCTCCATTCTTCA	AGGGACTGGTCACAGTGGTC
S50	55754893	T	C	BICF237J66607	TCTGCCTTTCTCCATTCTTCA	AGGGACTGGTCACAGTGGTC
S51	55754941	G	A		TCTGCCTTTCTCCATTCTTCA	AGGGACTGGTCACAGTGGTC
S52	55754981	T	A		TCTGCCTTTCTCCATTCTTCA	AGGGACTGGTCACAGTGGTC
S53	55755747	C	G		TGTCTTCATCCCTGTGAGGT	CCAGGAGGCATTTTCACACT
S54	55755801-55755803	GGG	Del		TGTCTTCATCCCTGTGAGGT	CCAGGAGGCATTTTCACACT
S55	55755864	C	T		TGTCTTCATCCCTGTGAGGT	CCAGGAGGCATTTTCACACT
S56	55786080	G	A		CTGGGACGGTTTGCATAAGT	CCTTAAATCACCCTGCCTCA
S57	55786273	G	A		CTGGGACGGTTTGCATAAGT	CCTTAAATCACCCTGCCTCA
S58	55836084	A	C	BICFPJ950727	TTCTCAGAGGAGGTGATGGG	CACTCTTGGCTTCTGTTCCC
S59	55872144	T	C	BICF235J38779	TTGAGAACTGTTCCGACGTG	AGGCTCCCCAGGTGTTTAGT
S60	55872165	T	C		TTGAGAACTGTTCCGACGTG	AGGCTCCCCAGGTGTTTAGT
S61	55877317	C	T	BICFPJ1486217	AAAACTGGTACACGGGGACA	CGATGTTCTCCAGCAGCATA
S62	55877321	C	T		AAAACTGGTACACGGGGACA	CGATGTTCTCCAGCAGCATA
S63	55877353	T	C		AAAACTGGTACACGGGGACA	CGATGTTCTCCAGCAGCATA
S64	55877420	C	T		AAAACTGGTACACGGGGACA	CGATGTTCTCCAGCAGCATA
S65	55877468	T	C	BICFPJ1486213	GCGGATGCTTTAGTGACCTG	GAGCACATTCCCGCTCTTAG
S66	55885068	G	A		ACTCCGGAGAGAGGTTCGAT	CTACCTGAGCCCCCACCTAC
S67	55885113	T	C	BICFPJ1052677	ACTCCGGAGAGAGGTTCGAT	CTACCTGAGCCCCCACCTAC
S68	55885114	G	A		ACTCCGGAGAGAGGTTCGAT	CTACCTGAGCCCCCACCTAC
S69	55896178	T	C	BICF235J38779	AGCTGACTCAACATGCAGGA	CCGTTCTATCTTCAGGGCAG
S70	55896184	T	C		AGCTGACTCAACATGCAGGA	CCGTTCTATCTTCAGGGCAG
S71	55896216	C	T		AGCTGACTCAACATGCAGGA	CCGTTCTATCTTCAGGGCAG
S72	55896221	A	G		AGCTGACTCAACATGCAGGA	CCGTTCTATCTTCAGGGCAG
S73	55896301	A	G		AGCTGACTCAACATGCAGGA	CCGTTCTATCTTCAGGGCAG
S74	56250053	G	A	BICF237J21474	GCGTGCTTTGCAGACATAAA	CCCACTGGATCTTCAGGTGT
S75	56525724	T	G	BICF231J21146	AGCTTTTCCTGAACACGCAT	CCGAGAGTTTTACAGCCGAG
S76	56525736	T	C		AGCTTTTCCTGAACACGCAT	CCGAGAGTTTTACAGCCGAG
S77	56525745	C	T		AGCTTTTCCTGAACACGCAT	CCGAGAGTTTTACAGCCGAG
S78	56525821	T	A		AGCTTTTCCTGAACACGCAT	CCGAGAGTTTTACAGCCGAG
S79	55746083	del	T		GCATGTACATCCACTAGGGACA	CAGTGATGTGGTGCTGTGTG
S80	55746221	C	T		GCATGTACATCCACTAGGGACA	CAGTGATGTGGTGCTGTGTG
S81	55746536	G	A		CCTTCTTGATTTTGCCCTCA	TTCCTTGGCTCTTCTCTCCA
S82	55746684-55746706	GA(…)TA	Del		CCTTCTTGATTTTGCCCTCA	TTCCTTGGCTCTTCTCTCCA
S83	55747087	A	G		GGACTACAGTGAAGGAGCCAAG	TGGAACCTCTCGGGAGACTA
S84	55747241	T	C		GGACTACAGTGAAGGAGCCAAG	TGGAACCTCTCGGGAGACTA
S85	55747266	A	C		GGACTACAGTGAAGGAGCCAAG	TGGAACCTCTCGGGAGACTA
S86	55747268	C	A		GGACTACAGTGAAGGAGCCAAG	TGGAACCTCTCGGGAGACTA
S87	55748067	G	A		GGGATCCTGGCTGGACTA	CTGTTGGGGAGGCCAACT

Table S2 (cont.): Polymorphisms used in the association study of the *K* locus

ID	CFA16 (bp) CanFam1.0	Tasha's allele	Other allele	Broad SNP ID	Primer Forward	Primer Reverse
S88	55748115	G	Del		GGGATCCTGGCTGGACTA	CTGTTGGGGAGGCCAACT
S89	55749774	A	C		ACAGGCTCGTCTGCTTGACT	TCTCTGGGCTAGGAGAAGCA
S90	55749950	T	C		ACAGGCTCGTCTGCTTGACT	TCTCTGGGCTAGGAGAAGCA
S91	55752630-55752632	TTT	Del		CCCCTCGTCAACCTTATCAA	TGAGCATCAGGTCACTGGAG
S92	55752862	G	A		TTGCCTTTAAAATGCCTTCC	AGCACAGGGCTATGGAAACA
S93	55752940	G	A		TTGCCTTTAAAATGCCTTCC	AGCACAGGGCTATGGAAACA
S94	55753338	G	T		TCTGAGGAAATTTTGCTTTTGA	AAGGGGCTTAGGAAGGTACG
S95	55754820	G	A		GGGTGAAGGAATCGCAAATA	TCCTTCAAGGGAATTGTTTGTT
S96	55757261	G	A		TCCATTGTCTCCAGTCTCCTG	GCGCTACTACAAAGGCAAGC
S97	55764041	G	A		ATGGTCTGCAGCACTCAGG	AAAATCGCAGGACAGAGCAT
S98	55764169	G	A		ATGGTCTGCAGCACTCAGG	AAAATCGCAGGACAGAGCAT
S99	55764190	C	T		ATGGTCTGCAGCACTCAGG	AAAATCGCAGGACAGAGCAT
S100	55765110-55765113	TATC	Del		AAGTCACAAAGGCAGGTTCC	CATGTCTCCTGAACCACAGG
S101	55765138	C	G		AAGTCACAAAGGCAGGTTCC	CATGTCTCCTGAACCACAGG
S102	55765233	C	T		AAGTCACAAAGGCAGGTTCC	CATGTCTCCTGAACCACAGG
S103	55765451	A	C		TGGCTACCAAATGGACACAG	GATCTTCTGCACCTTTCATGG
S104	55751487	G	A		CCCCACCTGCTCCTTACTCT	CATAGTCGAAGGGTGGCCTA
S105	55751488	C	A		CCCCACCTGCTCCTTACTCT	CATAGTCGAAGGGTGGCCTA

Table S3: Association of the coat color phenotype with *CBD103* genotype[a]

Breed	Genotype of pheomelaninistic dogs			Genotype of eumelanistic dogs		
	+/+	ΔG/+	ΔG/ΔG	+/+	ΔG/+	ΔG/ΔG
Afghan Hound	1				3	1
Akita	34					
Australian Shepherd	5				2	
Basenji	26				7	
Border Collie	2				1	1
Borzois	2					
Boxer	41					
Bulldog	27					
Bullmastiff	23					
Cavalier King Charles Spaniel	2					
Chow Chow	3				3	
Curly-Coated Retriever						5
Dalmatian						6
Doberman Pinsher	13					
Field Spaniel						5
Flat-Coated Retriever					3	1
French Brittany					1	
French Bulldog	1					
German Shepherd	7					
German Shorthaired Pointer						5
German Wirehaired Pointer						5
Great Dane	68				17	40
Greyhound	4				3	1
Havanese	1					
Irish Wolfhound	1					
Labrador Retriever					1	9
Large Munsterlander						3
Mastiff	7					
Miniature Doberman Pinsher	1					
Miniature Schnauzer	1					1
Poodle					2	3
Portuguese Water Dog						3
Pug	2					1
Puli	2				2	1
Rottweiler	10					
Shar-Pei	3				4	1
Weimaraner	2				4	4
Whippet	3					
Total	292	0	0	0	53	96

[a] Alleles are denoted as "+" for the reference sequence (since Tasha the Boxer is k^y/k^y) and "ΔG" for the 3 bp deletion (CFA16:55755801-55755803) referred to as S54 in Table S2, and which predicts the *CBD103*ΔG23 deletion described in the text. Not shown in this table are the genotypes of 13 dogs whose genotypes at *CBD103* were discordant with their coat color phenotype due to epistasis with *Mc1r* or *Agouti* mutations. Five "black" animals (in the German Shepherd Dog or Weimaraner breeds) were homozygous for a loss-of-function *Agouti* allele, and 8 "yellow" animals (in the Afghan Hound, French Bulldog, German Shorthaired Pointer, Labrador Retriever, Puli, or Poodle breeds) were homozygous for a loss-of-function *Mc1r* allele.

Figure S1

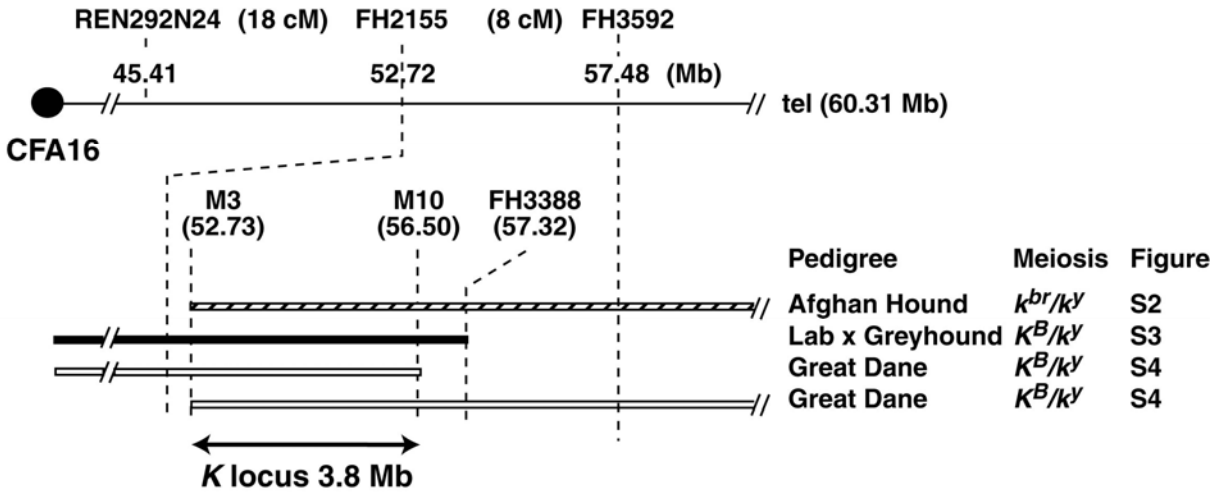

Figure S1. Genetic mapping of the *K* locus. The location of the *K* locus as determined by linkage analysis, with critical recombinant chromosomes from 3 pedigrees that define a minimal interval of 3.8 Mb. (In our original mapping studies (*16*), FH2155 cosegregated with K^{B}). Genetic markers (REN292N24, FH3592, FH2155, M3, M10, FH3388) are defined in Table S1 or (*4*), *K* locus genotype of key recombinant chromosomes are indicated as hatched (k^{br}), black (K^{B}) , or clear (k^{y}), with the meiosis and pedigree of origin indicated to the right.

Figure S2

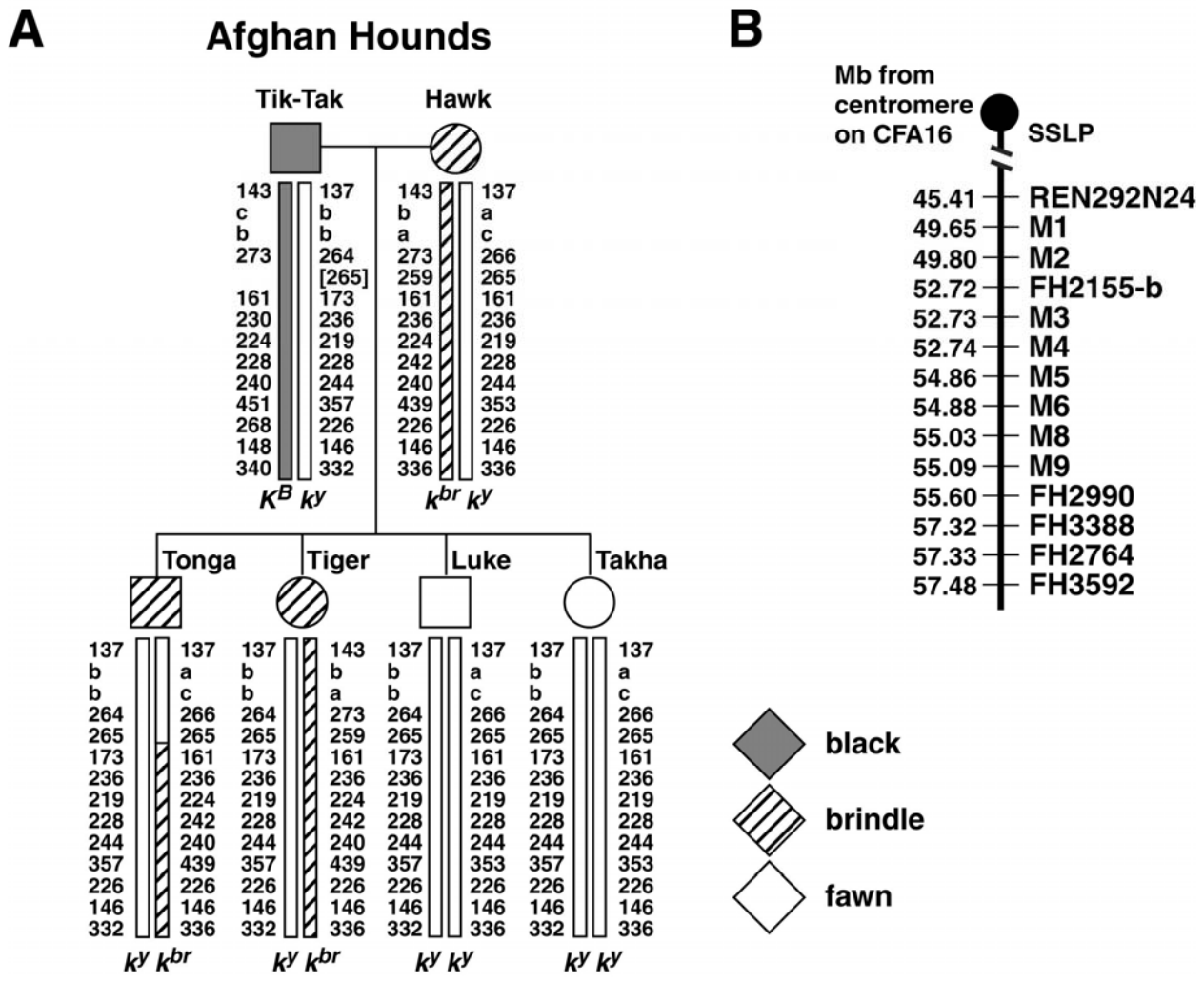

Figure S2. Haplotypes for a critical recombinant in an Afghan Hound pedigree. (A) Tonga carries a k^{br}-bearing recombinant chromosome transmitted from the mother that places the location of k^{br} distal to M3. Phase was inferred by assuming that most chromosomes are non-recombinant. Alleles are given as amplicon size for microsatellite loci as shown in (B), except for M1 and M2, for which alleles are lettered a, b, or c arbitrarily. Genotypes at the *K* locus were originally deduced from the pedigree, and later confirmed by genotyping for the ΔG23 mutation in *CBD103*; brackets denote genotypes that were not determined experimentally and instead inferred from the haplotype analysis.

Figure S3

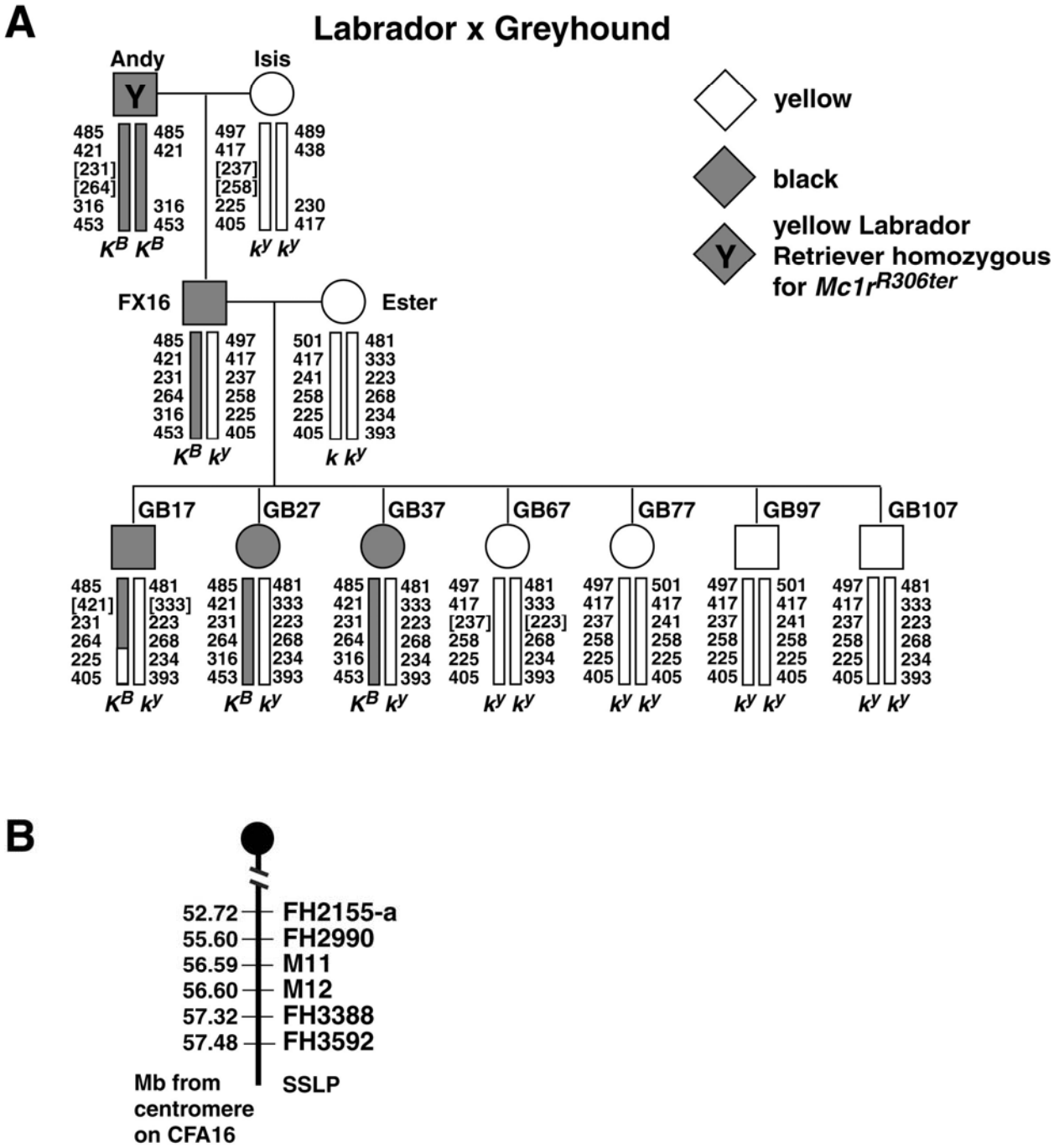

Figure S3. Haplotypes for a critical recombinant in a Labrador Retriever x Greyhound pedigree. (A) GB17 carries a K^B-bearing recombinant chromosome transmitted from the father that places the location of K^B proximal to FH3388. Symbols and conventions are as described in Figure S2, except for the phase at FH2155, FH2990, FH3388 and FH3592, which could be determined by pedigree analysis.

Figure S4

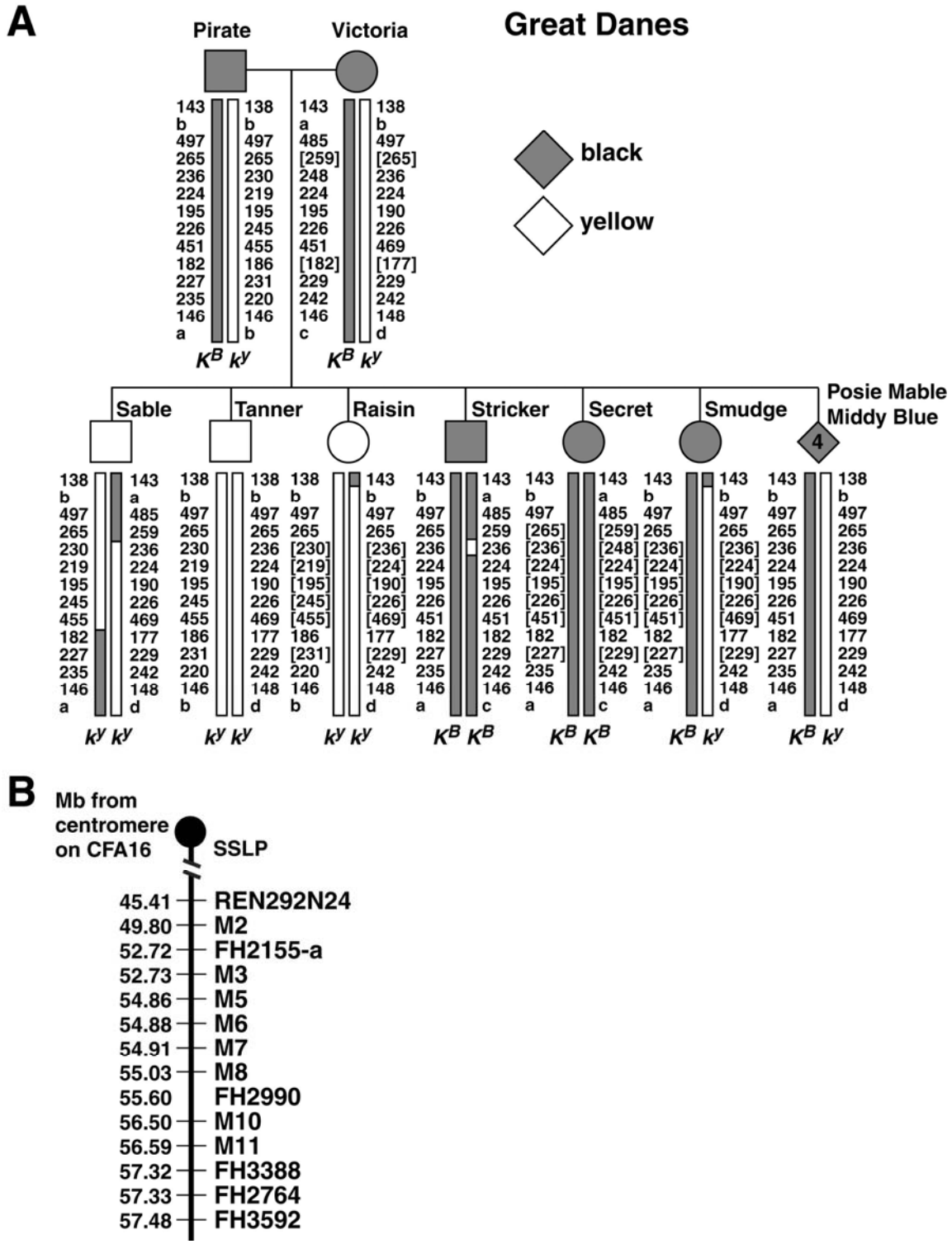

Figure S4. Haplotypes for critical recombinants in a Great Dane pedigree. (A) Sable carries two k^y-bearing recombinant chromosomes that place the location of k^y in a 3.8 Mb interval between M3 and M10. Symbols and conventions are as described in Figure S2.

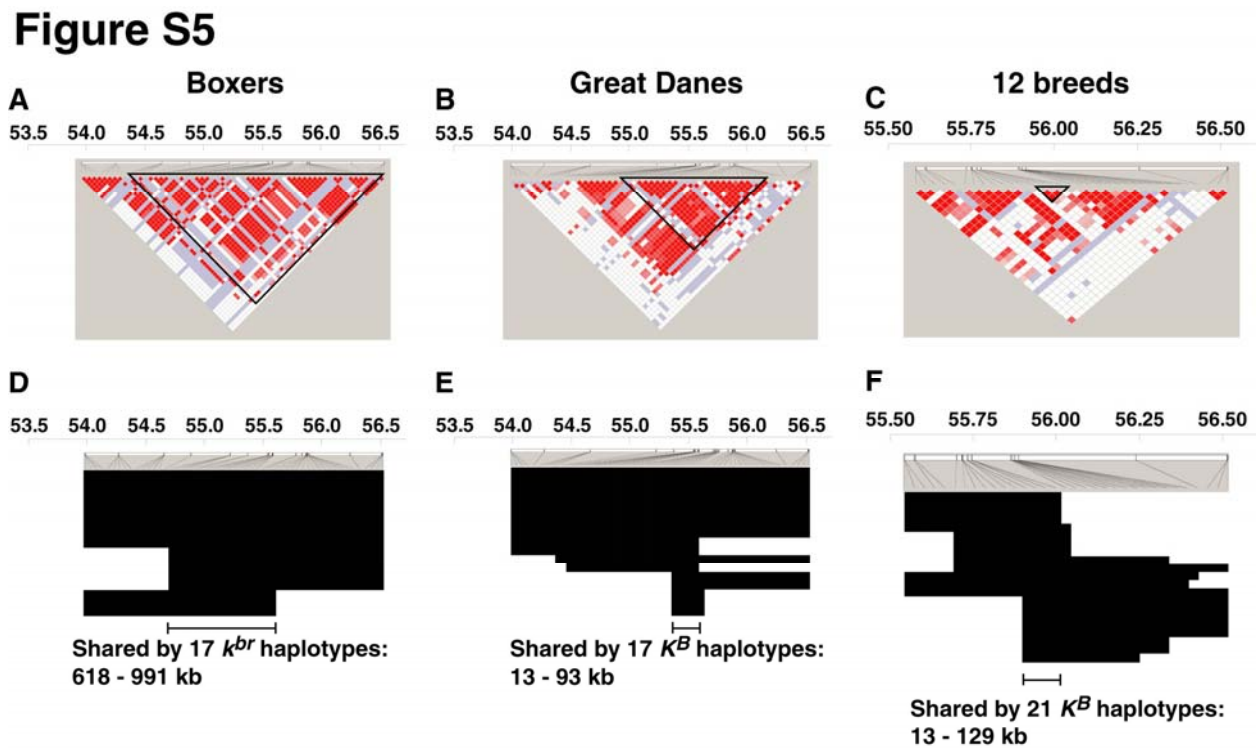

Figure S5. Haplotype analysis in Boxers, Great Danes, and multiple breeds. (A,B,C) Extent of LD between SNP pairs for each group as calculated by Haploview (red indicates D'= 1 and LOD >=2, pink indicates D'<1 and LOD>=2, blue indicates D'=1 and LOD<2, and white indicates D'<1 and LOD<2). Outlined in black is the block containing SNPs that pass the Bonferroni-corrected 5% significance threshold as indicated in Figure 1 for Boxers and Great Danes. In the 12 breed panel (C), 3 SNPs (outlined in black) were highly significant ($p < 10^{-6}$). (D,E,F) Haplotype sharing among non-k^{y} chromosomes in each group (k^{br} in Boxers, K^{B} in Great Danes and the 12 breed group). Haplotypes were estimated as described in the text and in Figures S9 and S10. For all panels, physical distance along CFA16 is given on the abscissa, only SNPs that were present at greater than 10% frequency and genotyped in at least 75% of the samples are shown.

Figure S6

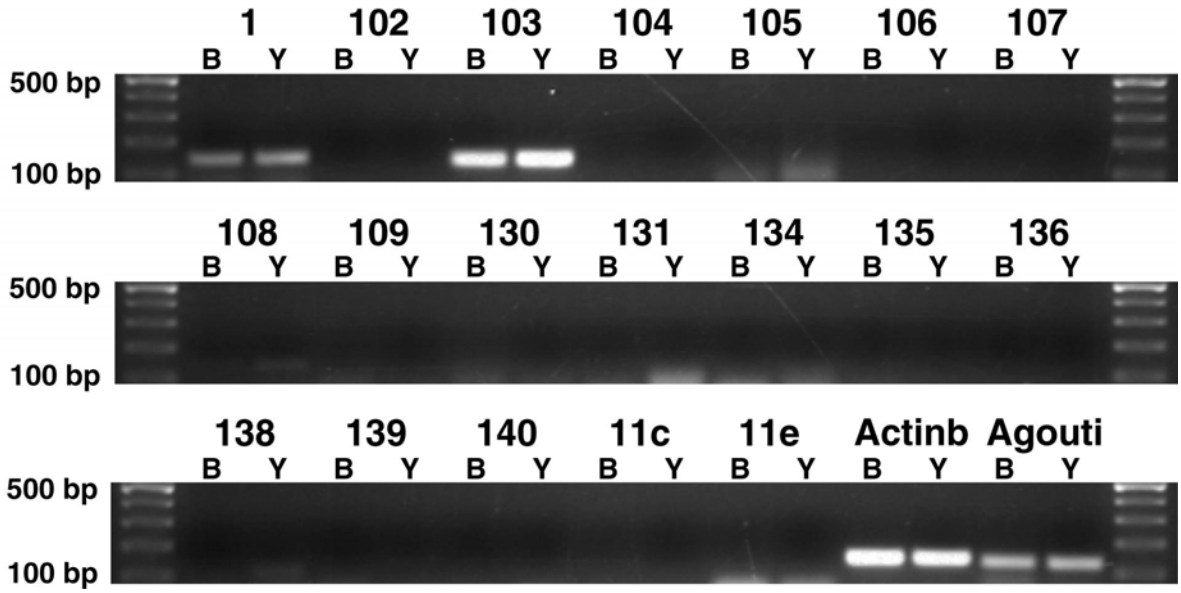

Figure S6. Expression of beta-defensin mRNA in dog skin. (A) Primer pairs for the indicated genes were used in an RT-PCR reaction with mRNA from a k^y/k^y (Y) and a K^B/k^y (B) dog.

Figure S7

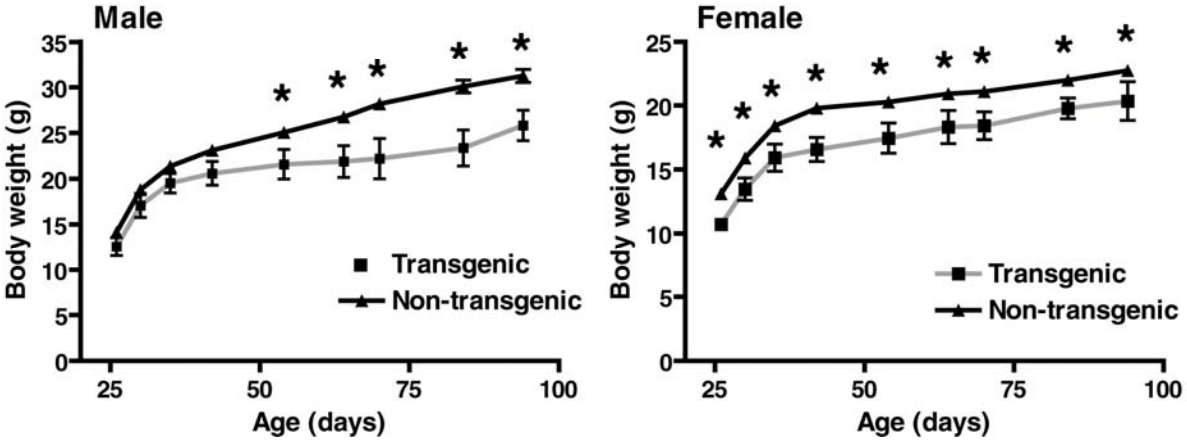

Figure S7. Effects of *CBD103* on weight gain in transgenic mice. Body weight for transgenic founders (males n=7; females n=4) compared to non-transgenic (males n=9; females n=16) littermates; asterisks indicate significant differences (t-test, $p < 0.05$).

Figure S8

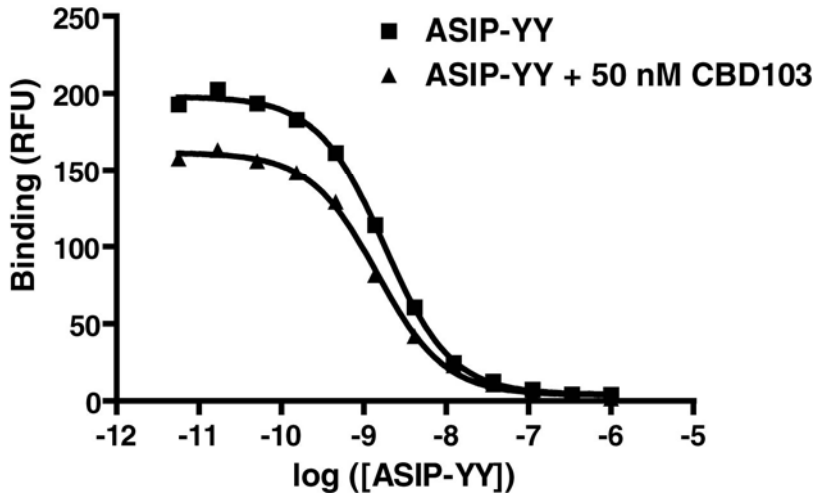

Figure S8. Binding displacement assay for ASIP-YY with and without 50 nM CBD103. ASIP-YY concentration is plotted on the abscissa as log of the molarity. The addition of CBD103 reduces the maximal binding and causes a slight leftward shift, indicating that ASIP-YY and CBD103 act in an additive manner to compete for Eu-NDP-MSH binding to the Mc1r.

Figure S9

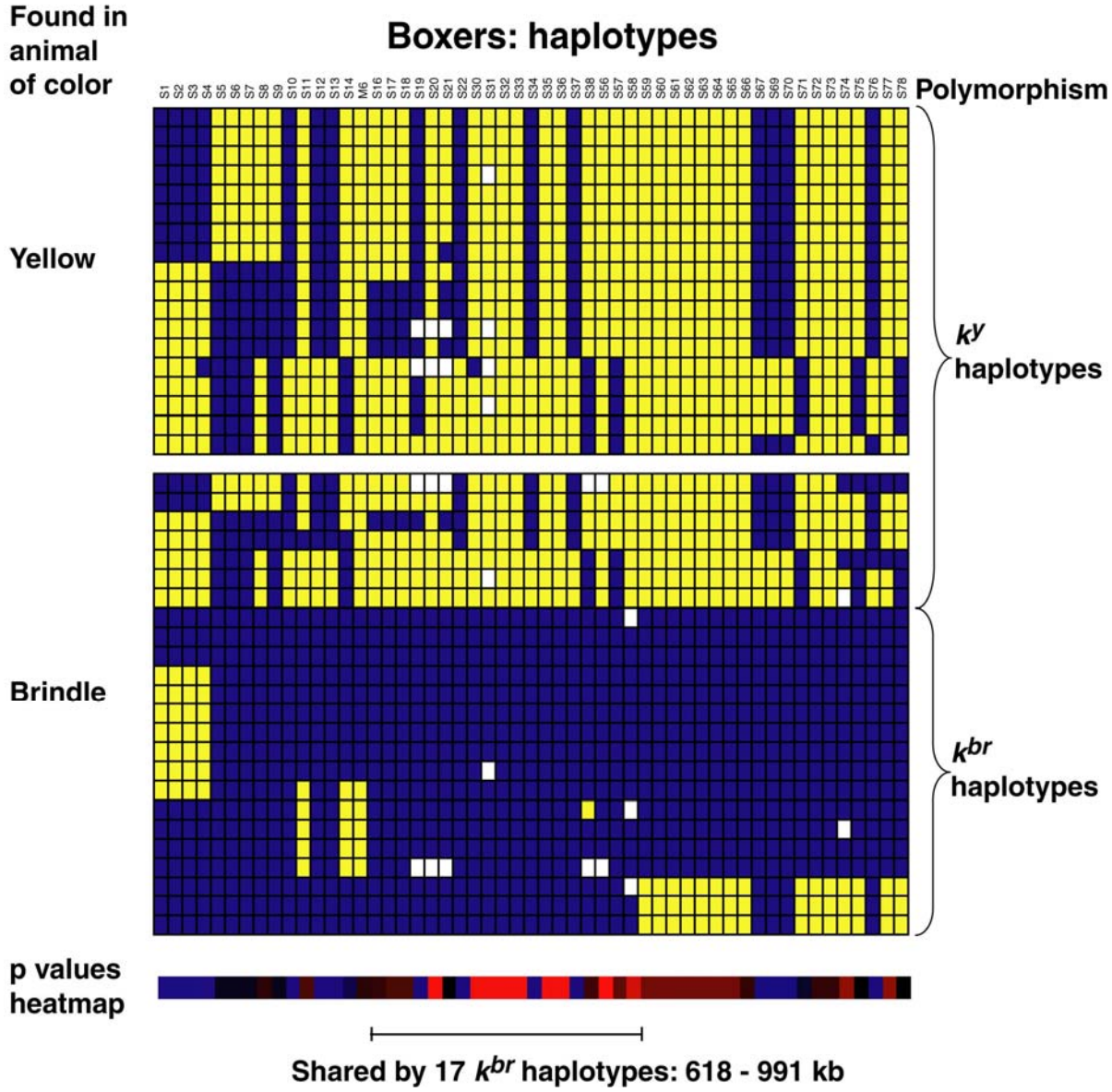

Figure S9. Long-range *K* locus haplotype structure in Boxers. Genotypes obtained for the association study depicted in Figure 1C were used to infer haplotypes; results are shown for 53 markers in 5 k^{br}/k^{br}, 7 k^{br}/k^{y}, and 9 k^{y}/k^{y} dogs, with some data excluded due to an unusual feature of the k^{br} mutation which will be described subsequently. Alleles found at highest frequency in brindle dogs are colored in blue; the other allele is colored in yellow, and missing data are colored in white. The k^{br} haplotypes are easily identified by a characteristic pattern of variation found in all dogs carrying one or two k^{br} alleles. For comparison to the association study, a heatmap for p values (whose values are shown in Figure 1C) is given at the bottom, where p values from the least to the greatest significance are colored from blue to red.

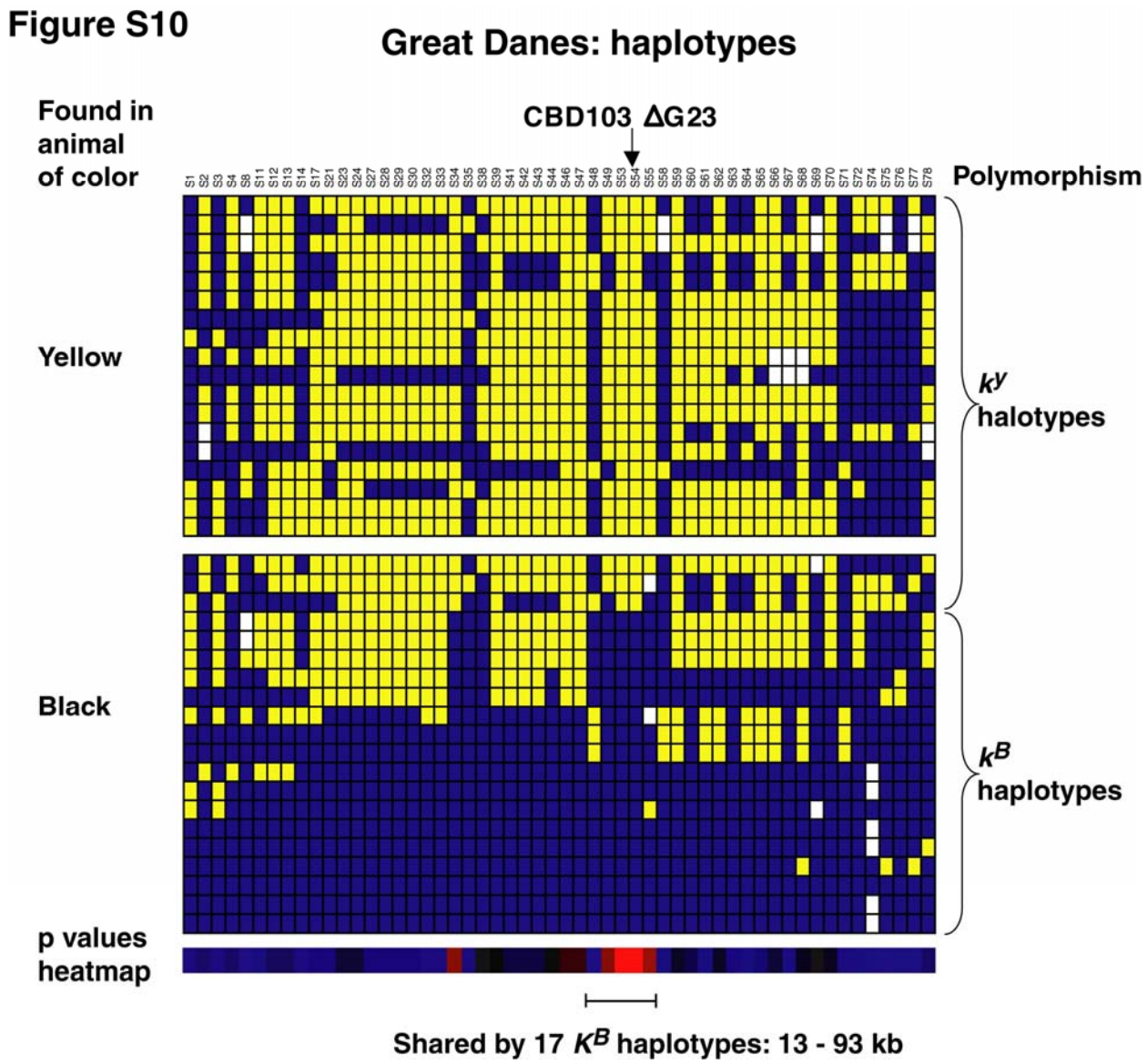

Figure S10. Long-range *K* locus haplotype structure in yellow and black Great Danes. Genotypes obtained for the association study depicted in Figure 1D together with 3 SNPs in *CBD103* were used to infer haplotypes in 7 K^B/K^B, 3 K^B/k^y, and 9 k^y/k^y dogs. Alleles found at highest frequency in black Great Danes are colored in blue; the other allele is colored in yellow, and missing data are colored in white. Unlike the situation that pertains in Boxers, K^B halotypes in Great Danes are not easily identified by a characteristic pattern of variation, and were assigned retrospectively (knowing that the cause of the K^B mutation is *CBD103*ΔG23). For comparison to the association study, a heatmap for p values (whose values are shown in Figure 1D) is given at the bottom, where p values from the least to the greatest significance are colored from blue to red.

References

1. D. Karolchik *et al.*, *Nucleic Acids Res* **31**, 51 (2003).
2. K. Lindblad-Toh *et al.*, *Nature* **438**, 803 (2005).
3. M. Neff, personal communication (2007).
4. R. Guyon *et al.*, *Proc Natl Acad Sci U S A* **100**, 5296 (2003).
5. M. Breen *et al.*, *BMC Genomics* **5**, 65 (2004).
6. I. Boutin-Ganache, M. Raposo, M. Raymond, C. F. Deschepper, *Biotechniques* **31**, 24 (2001).
7. J. M. Newton *et al.*, *Mamm Genome* **11**, 24 (2000).
8. J. A. Kerns *et al.*, *Mamm Genome* **15**, 798 (2004).
9. J. C. Barrett, B. Fry, J. Maller, M. J. Daly, *Bioinformatics* **21**, 263 (2005).
10. P. Scheet, M. Stephens, *Am J Hum Genet* **78**, 629 (2006).
11. M. Okabe, M. Ikawa, K. Kominami, T. Nakanishi, Y. Nishimune, *FEBS Lett* **407**, 313 (1997).
12. O. E. Sorensen *et al.*, *J Immunol* **174**, 4870 (2005).
13. J. C. McNulty *et al.*, *J Mol Biol* **346**, 1059 (2005).
14. Z. Wu *et al.*, *Proc Natl Acad Sci U S A* **100**, 8880 (2003).
15. D. C. Bennett, P. J. Cooper, I. R. Hart, *Int J Cancer* **39**, 414 (1987).
16. J. A. Kerns *et al.*, *Genetics* **176**, 1679 (2007).
17. T. G. Berryere, J. A. Kerns, G. S. Barsh, S. M. Schmutz, *Mamm Genome* **16**, 262 (2005).
18. D. J. Schibli *et al.*, *J Biol Chem* **277**, 8279 (2002).
19. B. Wilcox, C. Walkowicz, *The Atlas of Dog Breeds of the World*. (T.F.H. Publications, Neptune City, NJ, 1995).
20. www.ukboxerdogs.co.uk. (2007).